catalysts

MDPI

Article

Modified 7-Chloro-11*H*-Indeno[1,2-b]Quinoxaline Heterocyclic System for Biological Activities

Nakul Kumar [1,2], Gajendra Kumar Inwati [3], Emad M. Ahmed [4], Chhagan Lal [5], Bharat Makwana [3], Virendra K. Yadav [6], Saiful Islam [7], Hyun-Jo Ahn [8], Krishna K. Yadav [9] and Byong-Hun Jeon [8,*]

[1] School of Pure and Applied Sciences, Sabarmati University, Ahmedabad 380009, GJ, India; nakul.kumar@sabarmatiuniversity.edu.in
[2] School of Chemical Sciences, Central University of Gujarat, Gandhinagar 382030, GJ, India
[3] Department of Chemistry, HVHP Institute of Post Graduate Studies and Research, Sarva Vishwavidyalaya, Kadi 382715, GJ, India; gajendrainwati@gmail.com (G.K.I.); bhrtchem1@gmail.com (B.M.)
[4] Department of Physics, College of Science, Taif University, P.O. Box 11099, Taif 21944, Makkah, Saudi Arabia; e.makboul@tu.edu.sa
[5] Department of Chemistry, Harcourt Butler Technical University, Kanpur 208002, UP, India; clal9940@gmail.com
[6] Department of Microbiology, School of Sciences, P P. Savani University, Surat 394125, GJ, India; Yadava94@gmail.com
[7] Civil Engineering Department, College of Engineering, King Khalid University, Abha 61411, Asir, Saudi Arabia; sfakrul@kku.edu.sa
[8] Department of Earth Resources and Environmental Engineering, Hanyang University, Seoul 04763, Korea; hjahn93@hanyang.ac.kr
[9] Faculty of Science and Technology, Madhyanchal Professional University, Ratibad, Bhopal 462044, MP, India; envirokrishna@gmail.com
* Correspondence: bhjeon@hanyang.ac.kr

Citation: Kumar, N.; Inwati, G.K.; Ahmed, E.M.; Lal, C.; Makwana, B.; Yadav, V.K.; Islam, S.; Ahn, H.-J.; Yadav, K.K.; Jeon, B.-H. Modified 7-Chloro-11*H*-Indeno[1,2-b] Quinoxaline Heterocyclic System for Biological Activities. *Catalysts* **2022**, *12*, 213. https://doi.org/10.3390/catal12020213

Academic Editors: Wenshuai Zhu and Ming Zhang

Received: 28 December 2021
Accepted: 27 January 2022
Published: 11 February 2022

Abstract: Recent advances in functionalized organic Spiro heterocyclic compounds composed of nitrogen bonded five- and six-membered rings have been made, establishing them as a synthetic target in organic-based biomedical applications. In this work, we report a synthesis of spirocyclic compounds under a one-pot reaction using 1,3-dipolar cycloaddition in a regio and diastereoselective manner. The higher atomic economy with higher yield (95%) and regio and stereoselectivity were achieved by a multi-component reaction of L-proline (1), Indenoquinoxaline (2), and the dipolarophile of malononitrile (3) solvents followed by reflux conditions. The reaction intermediate comprised azomethineylides derived from reactive primary amines, and the spiro derivatives were synthesized up to a ≈ 95% yield. The structural and characteristic chemical components of the as-prepared Spiro compounds were characterized by ^{1}H-NMR, FTIR, and Mass spectroscopy. The functionalized spiro-pyrrolizidines were found to be effective for biological uses by considering their in vitro screening and antimicrobial impacts. Spiro constituents were found to be much more effective for Gram-positive bacteria due to the stronger lipophilic character of the molecules, and they resulted feasible membrane permeation in a biological system. Based on the planarity geometry of the Spiro pyrrolizidines, meta-substitution possesses steric hindrance and hence shows less effectiveness compared to para-substitution on the same nucleus, which shows a marginal steric effect. The biological studies showed that the derived spiro heterocyclic systems have an inhibitory effect of 50%.

Keywords: spiro heterocyclics; quinoxalin-11-one; one-pot synthesis; azomethineylides; biomedical uses

1. Introduction

Spiro pyrrolizidines have attracted much attention because of their multi-component processing and applicability towards multifunctional uses in the modern age of chemical

sciences and technologies. Spiro pyrrolizidines have been used to enhance antibacterial and anticancer activities by a number of studies in recent advances in organic molecular structures. The smooth strategies, synthetic efficacy, and biological relevance of functionalized organic substances such as fluoro-spiro-isoxazolines have implemented suitable anti-viral and anti-cancer agents. In this context, Liu, Dou, and Shi, [1] have suggested a single-step synthesis of dispiropyrrolidinebisoxindole derivatives with ≈ 85% yield using different chemical methods. Furthermore, the productivity of spiro pyrrolizidines was increased by up to 95% by Yang et al. [2], using the facile method. Rahmannejadi, Yavari, and Khabnadideh, 2020, also synthesized and evaluated a series of heterocyclic molecules for obtaining efficient antitumor agents. In another study, Selvakumar, Vaithiyanathan, and Shanmugam [3,4] also conducted the stereoselective synthesis of 3-spirocyclopentene- and 3-spiropyrazole-2-oxindoles via 1,3-dipolar cycloaddition reaction, followed by E- and Z-isomers of bromo derivatives with a ≈75% yield. Liu, Dou, and Shi, [5] and Barkov et al. [6] studied regio- and stereoselective 1,3-dipolar cycloaddition of indenoquinoxalinoneazomethineylides to achieve a larger amount of β-nitrostyrenes with 94% yield. Huang et al. [7] performed a one-pot reaction using isatin and sarcosine to synthesize different derivatives of dipolarophile 5-(4-bromobenzylidene)-1,3-dimethylpyrimidine-2,4,6-trione components. Meanwhile, Yang et al. [2] discussed the efficient regioselective synthesis of novel functionalized dispiropyrrolidines via a three-component (3 + 2) cycloaddition reaction with a yield of approximately 87%. Additionally, other studies have shown a desired synthetic route for Spiro indeno[1,2-b]quinoxaline-11,3′-pyrrolizidine derivatives [8]. These various approaches were considered for the higher yield of the final compounds including multicomponent derivatives of the heterocyclic Spiro compounds. However, a one-pot route was used to synthesize indenoquinoxalone Spiro pyrrolidine chromene-3-carbonitrile by Shachkus, Degutis, and Mikul'skis [9]. They considered that the electron-rich heterocyclic compounds have potential medicinal properties due to the presence of highly active binding sites on the molecular structures, which is why these functionalized molecules are widely used in the anticancer, antimalarial, antituberculosis, and progesterone sectors. In this work, we used acetonitrile medium to derive indeno[1,2-b]quinoxalin-11-one with a higher yield, followed by 1,3 dipolar addition. The used method is desirable for the synthesis of regioselective spiro moiety due to the easier handling and processing [10]. The synthesized spiro pyrrolizidine derivatives are nitrogen-containing heterocycles that play a vital role in medicinal chemistry because of their remarkable binding sites. 1,3-Dipolar cycloaddition of azomethineylides generated in situ from l-proline and indenoquinoxalinones moieties occurred at the aldehyde derivatives with malononitriles upon heating in acetonitrile, leading to the respective spirocyclic adducts with spiro substituent and the quinoxaline moiety. The azomethineylide represents one of the foremost reactive and versatile categories of 1,3-dipoles and is instantly trapped by a range of dipolarophiles forming substituted pyrrolidines. 1,3-dipolar cycloaddition reactions of azomethineylides have been well developed, and the reactions proceeded with high regio- and stereoselectivity [11].

2. Results and Discussion

Spiro pyrrolizidines reactions were completed within 3 h, and the resulted target structures were yielded up to 95%. This cascade reaction was efficiently promoted using the desired ortho-phenylene-1,2-diamine. Additionally, we explored this improved methodology for the synthesis of Spiro heterocyclic indeno[1,2-b]quinoxaline derivatives in acetonitrile by using chloroindenoquinoxaline (Scheme 1), which is a much more suitable chemical environment [1,2]. Our improved method for the synthesis of Spiro pyrrolidines indenoquinoxaline derivatives has merits because it includes reduced reaction time with a higher yield. It is noteworthy to mention that the polar solvents afforded an excellent yield compared to the non-polar ones. Excellent results were observed in the acetonitrile

solvent because of its polar aprotic nature with the polarity. This nature felicitates a miscible phase with water and a range of organic solvents, but not saturated hydrocarbons [12].

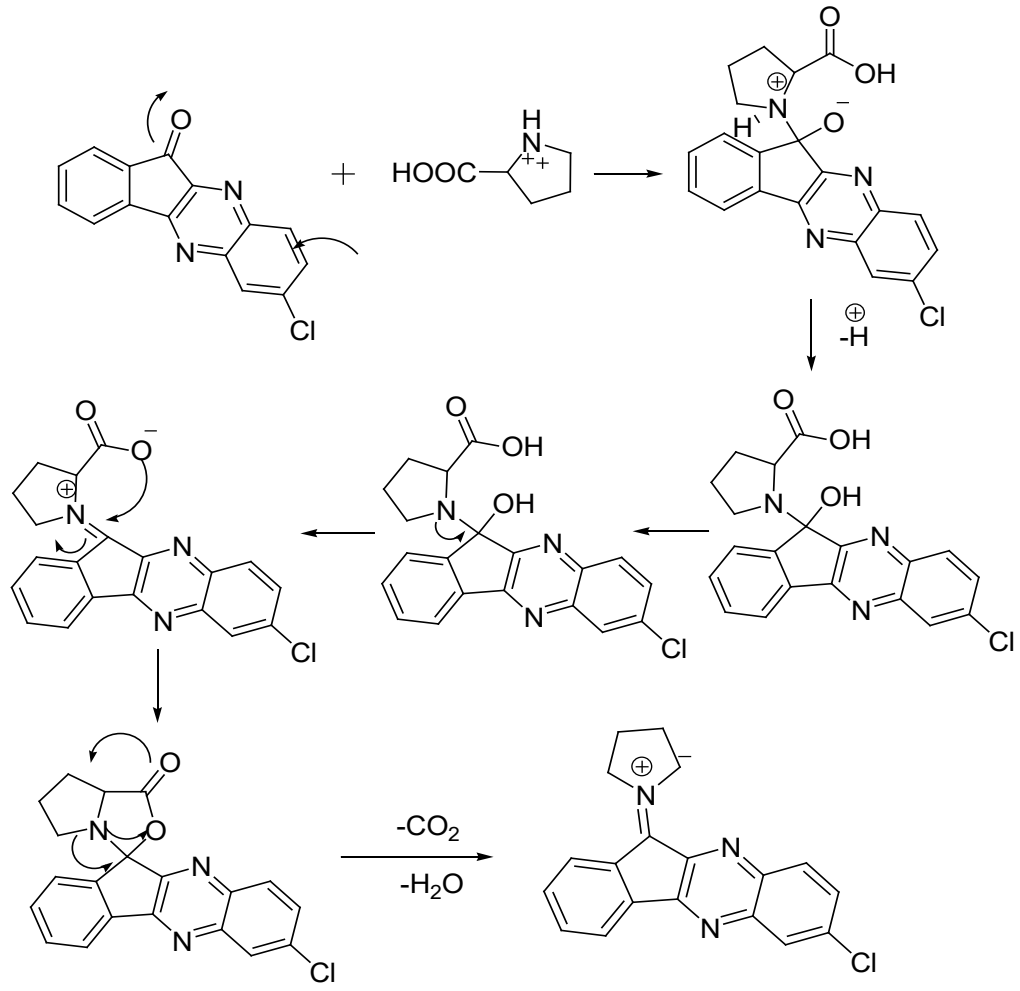

(a) Azomethine Ylide Formation from Chloroindiniquinoxaline and L-Proline

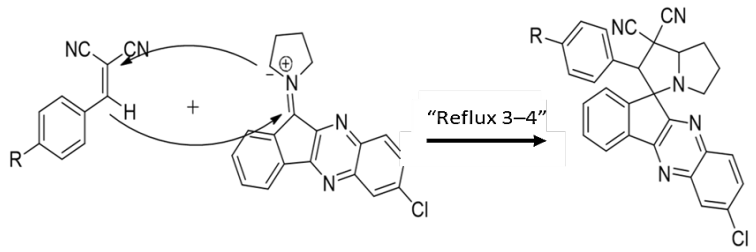

(b) Synthesis of Spiro Indenoquinoxaline from Azomethine Ylide and Starting material.
R = Cl, Br, F, CN, NO_2, OMe

Scheme 1. Proposed schematic mechanism of the synthesis of Spiro derivatives. (**a**) Mechanism for Azomethine formation, (**b**) Scheme for spiro indenoquinoxaline.

Spiro derivatives were prepared by an asymmetric 1,3-dipolar cycloaddition between chloroindenoquinoxaline and the starting materials (a product of malononitrile and aldehydes). Preliminarily, the reaction of the Spiro pyrrolizidines derivative I–VIII was carried out in acetonitrile solvents using chloroindenoquinoxaline and L-Proline under reflux for 3 h. The afforded moderate yield for Spiro I—86%, Spiro II—84%, Spiro III—

79%, Spiro IV—83%, Spiro V—87%, Spiro VI—95%, Spiro VII—89%, and Spiro VIII—91% were obtained. In this context, Huang et al. [13] reported decorated Spiro pyrrolidines derivatives by incorporating both the bioactive moieties in a single structural framework. Tan et al. [14] have studied an efficient synthesis of 9-anthrone lactone derivatives via Knoevenagel condensation towards efficient biological applications. However, in the present scenario, we introduced a facile method to prepare the Spiro pyrrolidines and Spiro pyrrolizidines derivatives under a 1,3-dipolar cycloaddition reaction [15,16].

2.1. NMR and Mass Spectral Analysis for Synthesized Spiro Compounds (I-VIII)

Spiro I: 7-chloro-2′-phenyl-7′,7a′-dihydrospiro[indeno[1,2-b]quinoxaline-11,3′-pyrrolizine]-1′,1′(2′H)-dicarbonitrile, shown in Scheme 2.

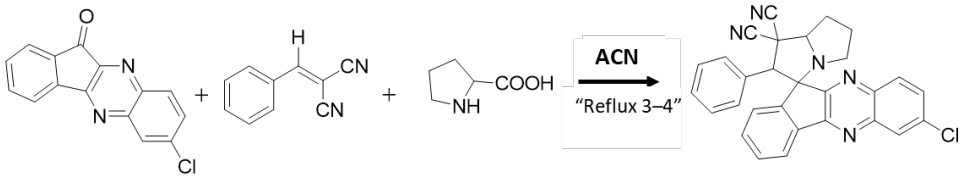

Scheme 2. 7-chloro-2′-phenyl-7′,7a′-dihydrospiro[indeno[1,2-b]quinoxaline-11,3′-pyrrolizine]-1′,1′(2′H)-dicarbonitrile.

Color, dark yellow solid; Yield, 86%; ^{1}H-NMR, 500 MHz ($CDCl_3$). The ^{1}H-NMR spectral data of the Spiro I compound is shown in Figure 1a. The observed structural NMR parameters are as follows: δ_H-ppm: 8.58, (s, 1H), 8.21, (d, 1H J = 8.49), 8.13 (d, 1H J = 8.71), 7.93(m, 1H J = 7.57), 7.71 (m, 1H J = 7.65), 7.46 (m, 1H J = 7.83), 6.96 (s, 1H), 6.86 (d, 1H), 6.76 (s, 1H), 5.36 (d, 1H J = 9.73), 5.12 (s, 1H), 4.68 (m, 1H J = 8.63), 4.12 (t, 1H J = 7.23), 3.94 (s, 1H), 2.69 (d 1H J = 7.40), 1.63 (s, 1H), 1.37-1.14 (m, 1H J = 7.34), 0.87, (s, 1H). The MS spectral data are f m/z 474.1991 (m + 1) for the as-prepared material, and the spectrum is presented in Figure 1b.

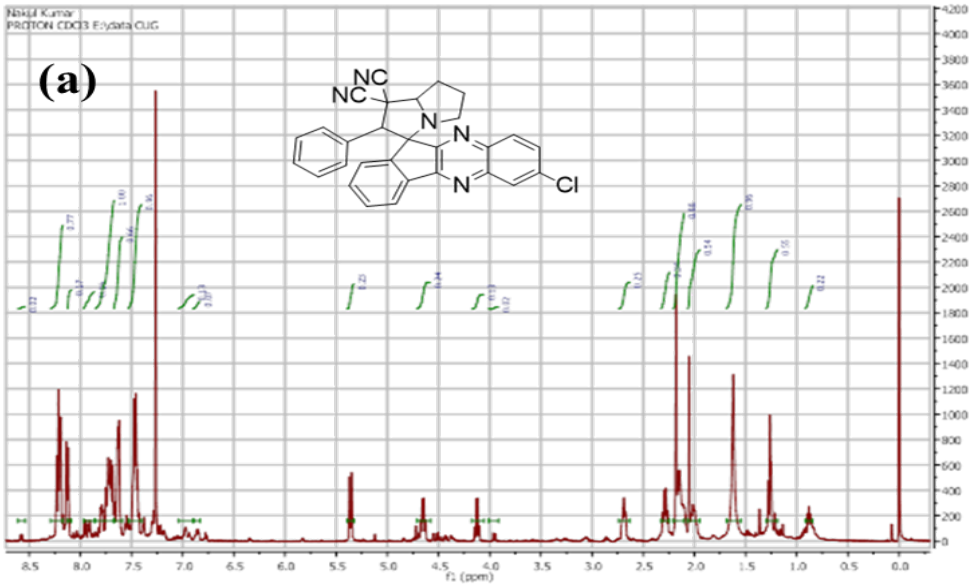

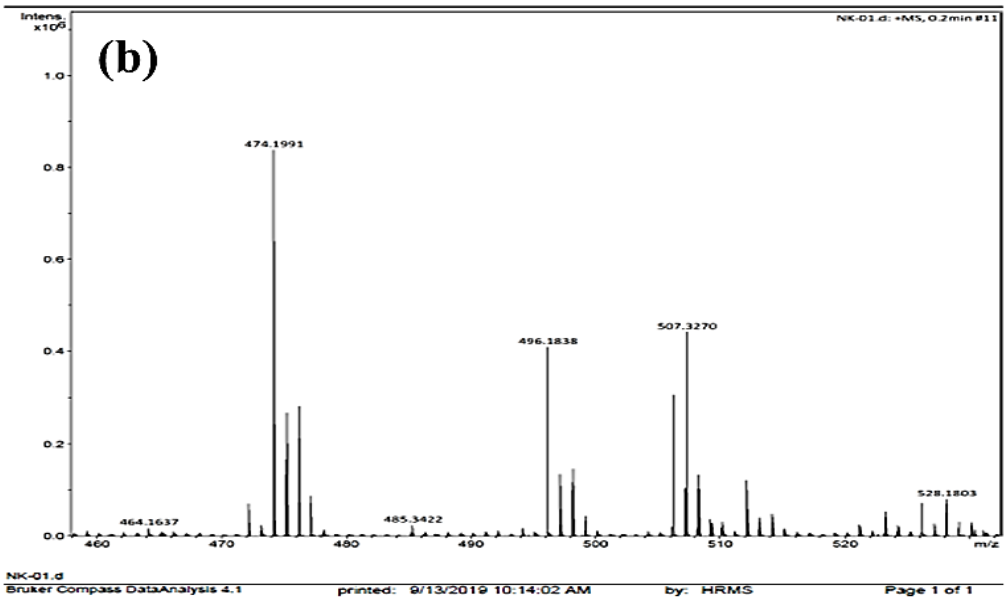

Figure 1. (**a**) NMR spectra for 7-chloro-2′-phenyl-7′,7a′-dihydrospiro[indeno[1,2-b]quinoxaline-11,3′-pyrrolizine]-1′,1′(2′H)-dicarbonitrile and (**b**) MS spectra for Spiro I.

Spiro II: 7-chloro-2′-(4-fluorophenyl)-7′,7a′-dihydrospiro [indeno [1,2-b]quinoxaline-11,3′-pyrrolizine]-1′,1′(2′H)-dicarbonitrile, Scheme 3.

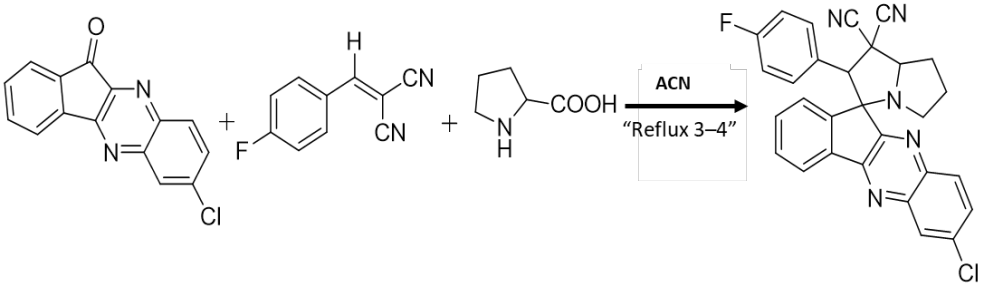

Scheme 3. Synthesis mechanism for 7-chloro-2′-(4-fluorophenyl)-7′,7a′-dihydrospiro [indeno [1,2-b]quinoxaline-11,3′-pyrrolizine]-1′,1′(2′H)-dicarbonitrile.

Color; light yellow solid; Yield, 84%; ^{1}H-NMR, 500 MHz ($CDCl_3$). The ^{1}H-NMR spectral data of the Spiro II compound is shown in Figure 2a. The obtained NMR parameters are as follows: δ_H-ppm: 8.20 (d, 1H *J* = 6.62), 8.13 (s, 1H), 7.81 (t, 1H *J* = 8.57), 7.70 (s, 1H), 7.40 (d, 1H *J* = 7.41), 7.35 (d, 1H *J* = 8.63), 7.14 (t, 1H *J* = 6.30), 6.97 (d, 1H *J* = 7.5), 6.19 (s, 1H), 5.36 (d, 1H *J* = 9.63), 5.31 (s, 1H), 4.81 (d, 1H *J* = 5.65), 4.72 (s, 1H), 4.59 (d, 1H *J* = 7.51), 4.46 (d, 1H *J* = 9.95), 4.42 (s, 1H), 4.35 (d, 1H *J* = 5.08), 3.88 (d, 1H *J* = 10.98), 3.56 (d, 1H *J* = 10.20), 3.30 (d, 1H *J* = 6.61), 2.85 (s, 1H), 2.68 (d, 1H *J* = 8.71), 2.29 (m, 1H), 2.15 (d, 1H *J* = 7.09), 2.04 (s, 1H). The MS spectral line of m/z 492.1381(m ± 1) is presented in Figure 2b.

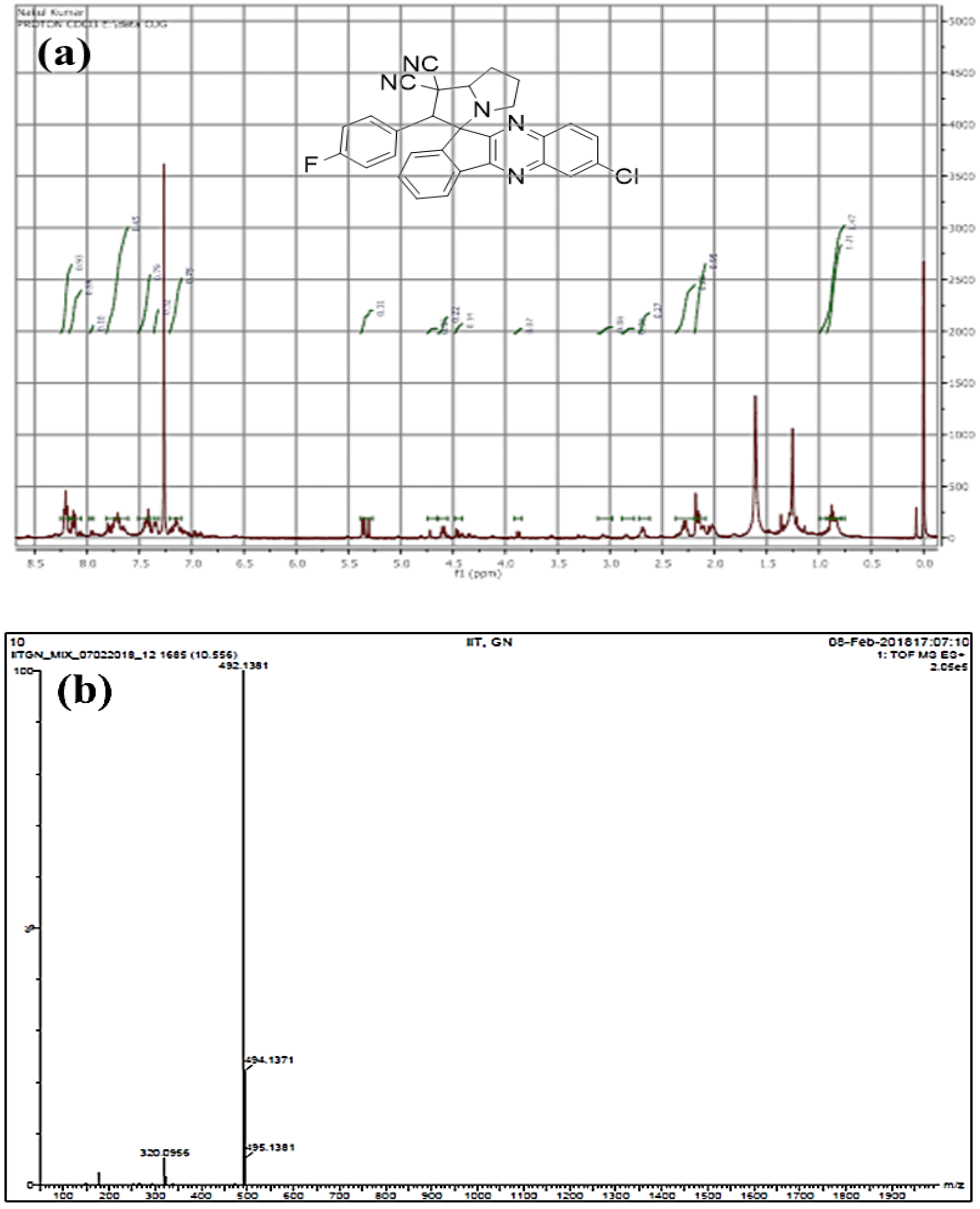

Figure 2. (**a**) 7-chloro-2′-(4-fluorophenyl)-7′,7a′-dihydrospiro[indeno[1,2-b]quinoxaline-11,3′-pyrrolizine]-1′,1′(2′H)-dicarbonitrile and (**b**) MS spectrum for Spiro II.

Spiro III: 2′-(3-bromophenyl)-7-chloro-5′,6′,7′,7a′-tetrahydrospiro[indeno[1,2-b]quinoxaline-11,3′-pyrrolizine]-1′,1′(2′H)-dicarbonitrile, Scheme 4.

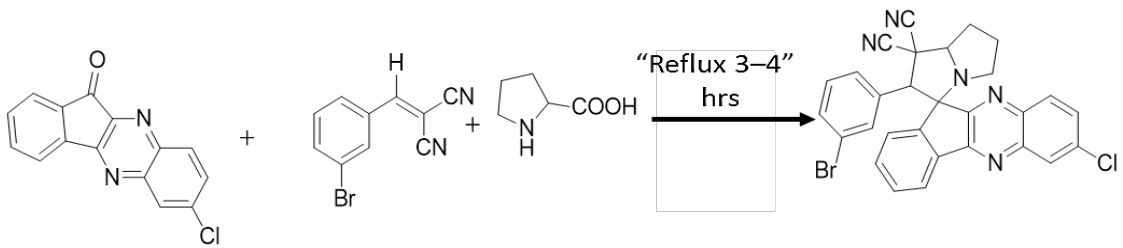

Scheme 4. Synthesis mechanism for 2′-(3-bromophenyl)-7-chloro-5′,6′,7′,7a′-tetrahydrospiro[indeno[1,2-b]quinoxaline-11,3′-pyrrolizine]-1′,1′(2′H)-dicarbonitrile.

Color; dark yellow solid; Yield, 79%; ^{1}H-NMR, 500 MHz ($CDCl_3$) The ^{1}H-NMR spectral data of the Spiro III compound is shown in Figure 3a. The obtained NMR parameters

are as follows: δ_H-ppm: 8.20 (d, 1H *J* = 8.31), 8.12 (m, 1H *J* = 9.08), 7.96 (d, 1H *J* = 7.28), 7.81 (t, 1H *J* = 8.49), 7.72 (s, 1H), 7.62 (d, 1H *J* = 7.88), 7.50 (d, 1H *J* = 8.62), 7.35 (d, 1H *J* = 8.29), 7.16 (t, 1H *J* = 8.56), 5.31 (d, 1H *J* = 9.31), 4.59 (d, 1H *J* = 8.58), 4.41 (d, 1H *J* = 10.31), 4.29 (m, 1H *J* = 5.94), 3.81 (t, 1H *J* = 10.98), 3.52 (d, 1H *J* = 10.03), 3,21 (s, 1H), 3 (s, 1H), 2.68 (t, 1H *J* = 6.42), 2.27 (m, 1H *J* = 8.83), 0.87 (d, 1H *J* = 6.25). The value of MS, m/z 554.1189(m ± 1), is shown in Figure 3b.

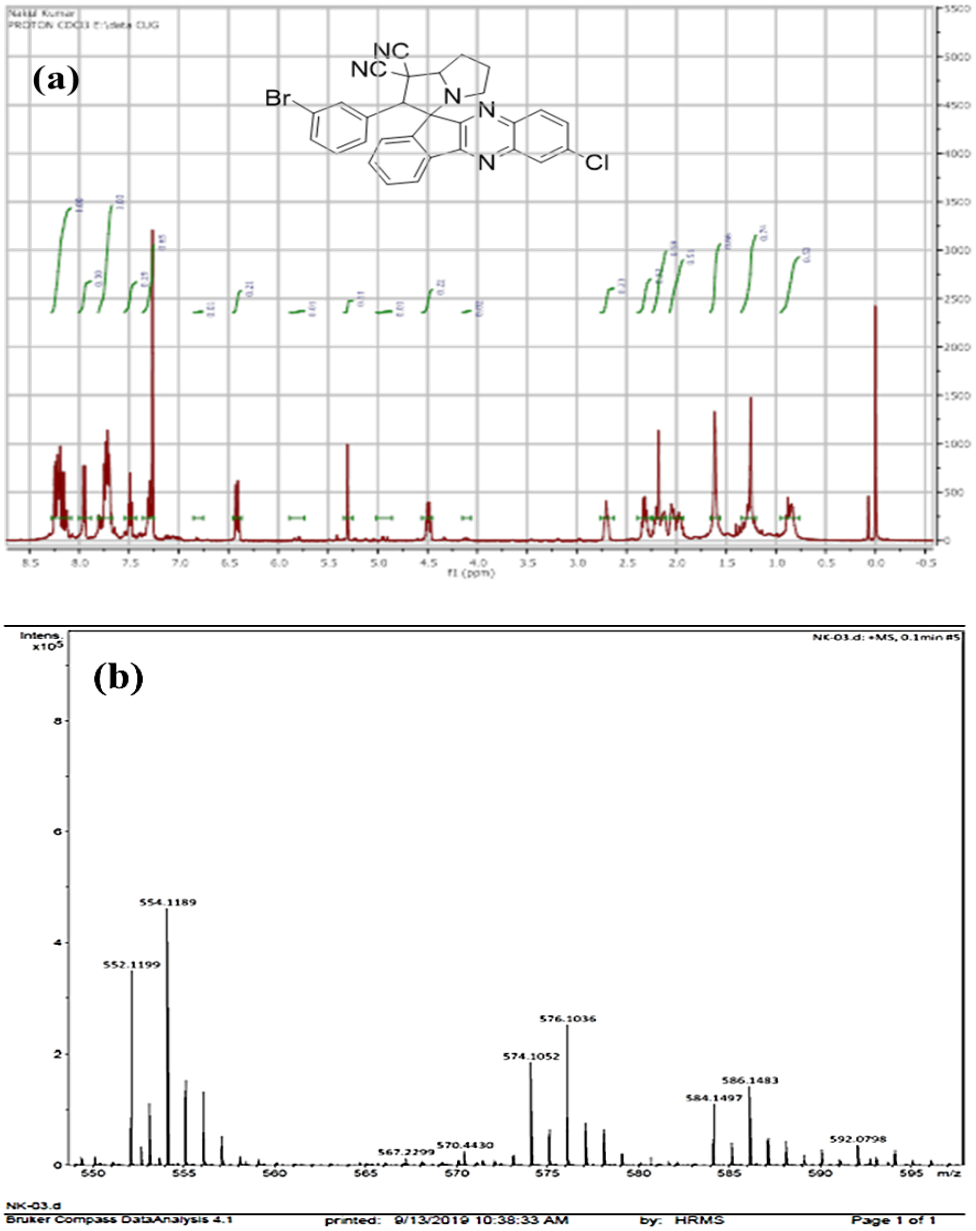

Figure 3. (**a**) 2′-(3-bromophenyl)-7-chloro-5′,6′,7′,7a′-tetrahydrospiro[indeno[1,2-b]quinoxaline-11,3′-pyrrolizine]-1′,1′(2′H)-dicarbonitrile and (**b**) MS spectrum for Spiro III.

Spiro IV: 2′-(4-bromophenyl)-7-chloro-5′,6′,7′,7a′-tetrahydrospiro[indeno[1,2-b]quinoxaline-11,3′-pyrrolizine]-1′,1′(2′H)-dicarbonitrile, Scheme 5.

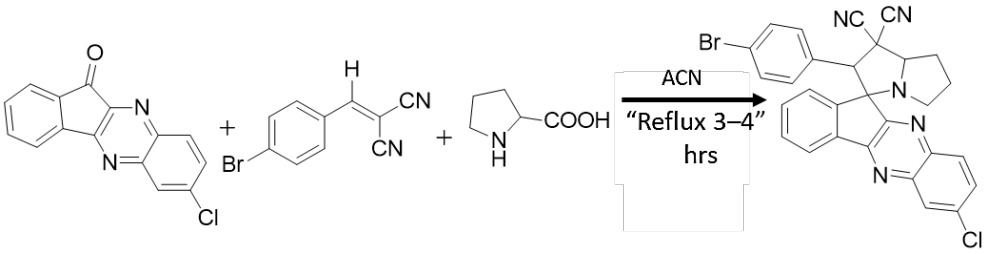

Scheme 5. Synthesis mechanism for 2′-(4-bromophenyl)-7-chloro-5′,6′,7′,7a′-tetrahydrospiro[indeno[1,2-b]quinoxaline-11,3′-pyrrolizine]-1′,1′(2′H)-dicarbonitrile.

Color, yellow solid; Yield, 83%; ^{1}H-NMR, 500 MHz ($CDCl_3$). The ^{1}H-NMR spectral data of the Spiro IV compound is shown in Figure 4a. The obtained NMR parameters are as follows: δ_H-ppm: 8.24 (d, 1H *J* = 7.70), 8.21 (m, 2H *J* = 6.09), 8.16 (d, 1H *J* = 8.85), 8.13 (d, 1H *J* = 8.85), 7.95 (d, 1H *J* = 7.84), 7.79 (d, 1H *J* = 9.30), 7.72 (m, 4 h *J* = 7.78), 7.49 (t, 1H *J* = 7.60), 7.29 (t, 1H *J* = 7.67), 6.82 (d, 1H *J* = 7.90), 6.41 (m, 1H *J* = 9.61), 5.84 (s, 1H), 5.79 (d, 1H *J* = 5.76), 5.49 (s, 1H), 5.23 (d, 1H *J* = 8.52), 5.05 (s, 1H), 4.95 (s, 1H), 4.91 (s, 1H), 4.49 (d, 1H *J* = 8.05) 4.33 (d, 1H *J* = 6.33), 3.19 (s, 1H), 2.71(t, 1H *J* = 10.18), 2.31 (m, 1H *J* = 8.36), 2.04 (s, 1H). The MS, m/z 554.1189 (m ± 1), is displayed in Figure 4b.

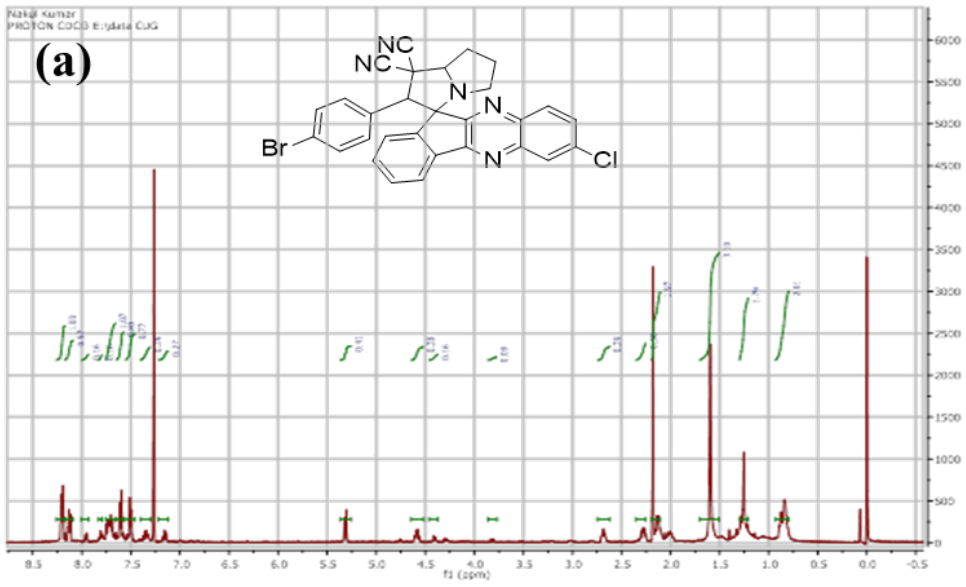

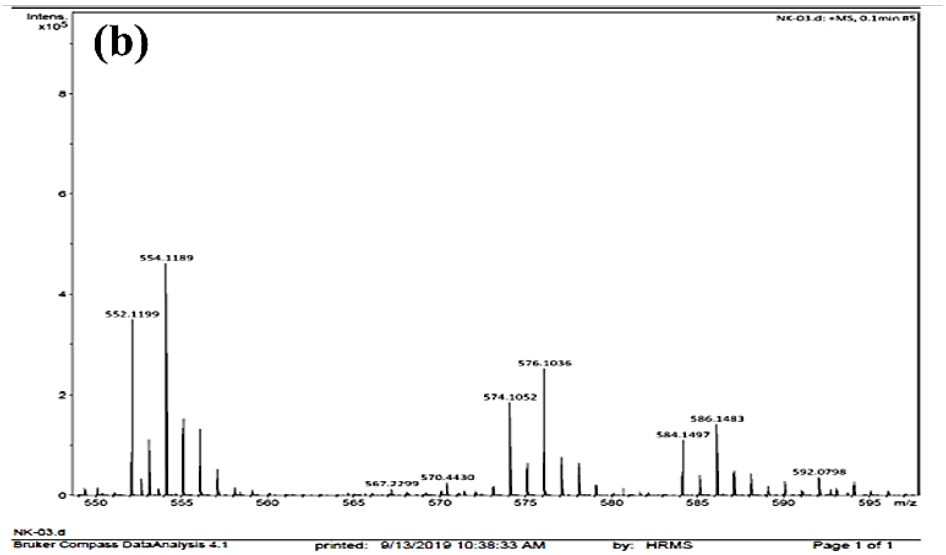

Figure 4. (**a**) 2′-(4-bromophenyl)-7-chloro-5′,6′,7′,7a′-tetrahydrospiro[indeno[1,2-b]quinoxaline-11,3′-pyrrolizine]-1′,1′(2′H)-dicarbonitrile and (**b**) MS spectrum for Spiro VI.

Spiro V: 7-chloro-2′-(4-chlorophenyl)-5′,6′,7′,7a′-tetrahydrospiro[indeno[1,2-b]quinoxaline-11,3′-pyrrolizine]-1′,1′(2′H)-dicarbonitrile, Scheme 6.

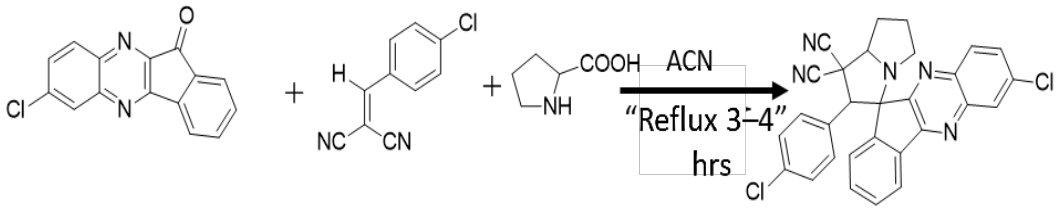

Scheme 6. 7-chloro-2′-(4-chlorophenyl)-5′,6′,7′,7a′-tetrahydrospiro[indeno[1,2-b]quinoxaline-11,3′-pyrrolizine]-1′,1′(2′H)-dicarbonitrile.

Color, light yellow solid; Yield, 87%; ^{1}H-NMR, 500 MHz ($CDCl_3$). The ^{1}H-NMR spectral data of the Spiro V compound is shown in Figure 5a. The obtained NMR parameters are as follows: δ_H-ppm: 8.57 (t, 1H *J* = 7.71), 8.30 (d, 1H *J* = 7.39), 8.20 (m, 1H *J* = 7.47), 8.16 (s, 1H), 8.13 (t, 1H *J* = 8.50), 8.07 (s, 1H), 7.95 (d, 1H *J* = 7.69), 7.80 (t, 1H *J* = 7.67), 7.72 (s, 1H), 7.65 (s, 1H), 7.57 (d, 1H *J* = 7.39), 7.46 (m, 1H *J* = 8.30), 7.38 (s, 1H), 7.21 (s, 1H), 7.05 (s,1H), 6.86 (s, 1H), 6.79 (d, 1H *J* = 7.02), 6.62 (t, 1H *J* = 8.22), 5.41 (s, 1H), 5.33 (d, 1H *J* = 9.69), 5.00 (s, 1H), 4.70 (s, 1H), 4.59 (d, 1H *J* = 8.65), 4.43 (s, 1H), 3.83 (m, 1H *J* = 10.89), 3.53 (t, 1H *J* = 10.29), 2.68 (d, 1H *J* = 8.45), 2.28 (d, 1H *J* = 6.58), 2 (s, 1H). The spectral MS, m/z 508.1341 (m ± 1), is shown in Figure 5b.

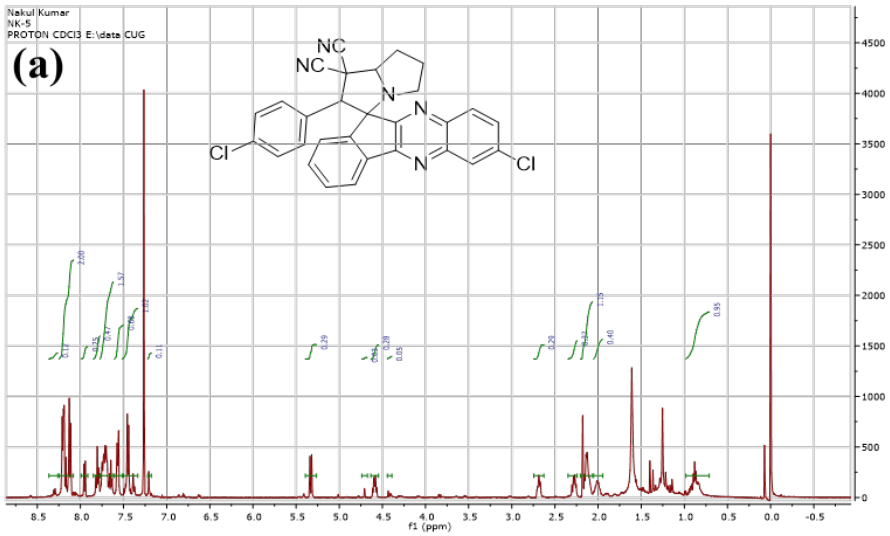

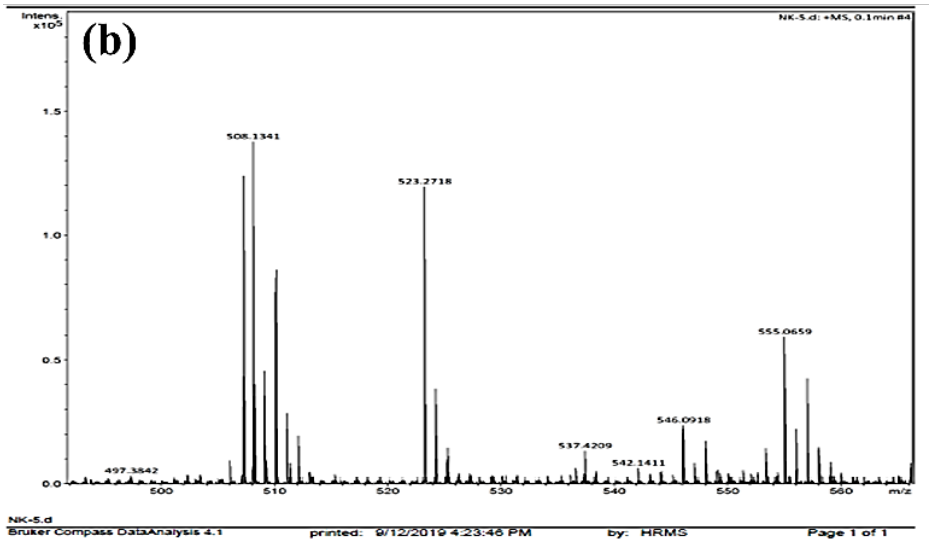

Figure 5. (**a**) 7-chloro-2′-(4-chlorophenyl)-5′,6′,7′,7a′-tetrahydrospiro[indeno[1,2-b]quinoxaline-11,3′-pyrrolizine]-1′,1′(2′H)-dicarbonitrile and (**b**) MS spectrum for Spiro V.

Spiro VI: 7-chloro-2′-(4-methoxyphenyl)-5′,6′,7′,7a′-tetrahydrospiro[indeno[1,2-b]quinoxaline-11,3′-pyrrolizine]-1′,1′(2′H)-dicarbonitrile, Scheme 7.

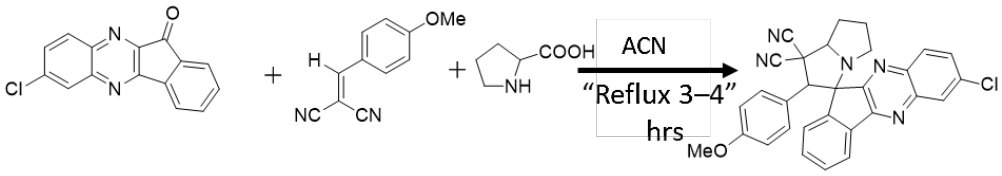

Scheme 7. Synthesis mechanism for7-chloro-2′-(4-methoxyphenyl)-5′,6′,7′,7a′-tetrahydrospiro[indeno[1,2-b]quinoxaline-11,3′-pyrrolizine]-1′,1′(2′H)-dicarbonitrile.

Color; light yellow solid; Yield, 95%; ^{1}H-NMR, 500 MHz ($CDCl_3$). The ^{1}H-NMR spectral data of the Spiro VI compound is shown in Figure 6a. The obtained values are as follows: δ_H-ppm: 8.20 (d, 1H *J* = 8.99), 8.13 (d, 1H *J* = 8.69), 7.95 (d, 1H *J* = 7.51), 7.81 (t, 1H *J* = 7.37), 7.66 (d, 1H *J* = 7.35), 7.55 (d, 1H *J* = 8.41), 7.22 (s, 1H), 6.99 (d, 1H *J* = 8.44), 5.30 (d, 1H *J* = 9.52), 4.60 (d, 1H *J* = 8.62), 3.90 (t, 1H *J* = 8.94), 2.67 (d, 1H *J* = 7.64), 2.28 (d, 1H *J* = 6.71), 2.17 (s, 1H), 2.13 (s, 1H), 1.99 s, 1H), 1.27 (s, 1H), 0.87 (d, 1H *J* = 6.73). The spectral MS, m/z 502.3625 (m ± 1), is shown in Figure 6b.

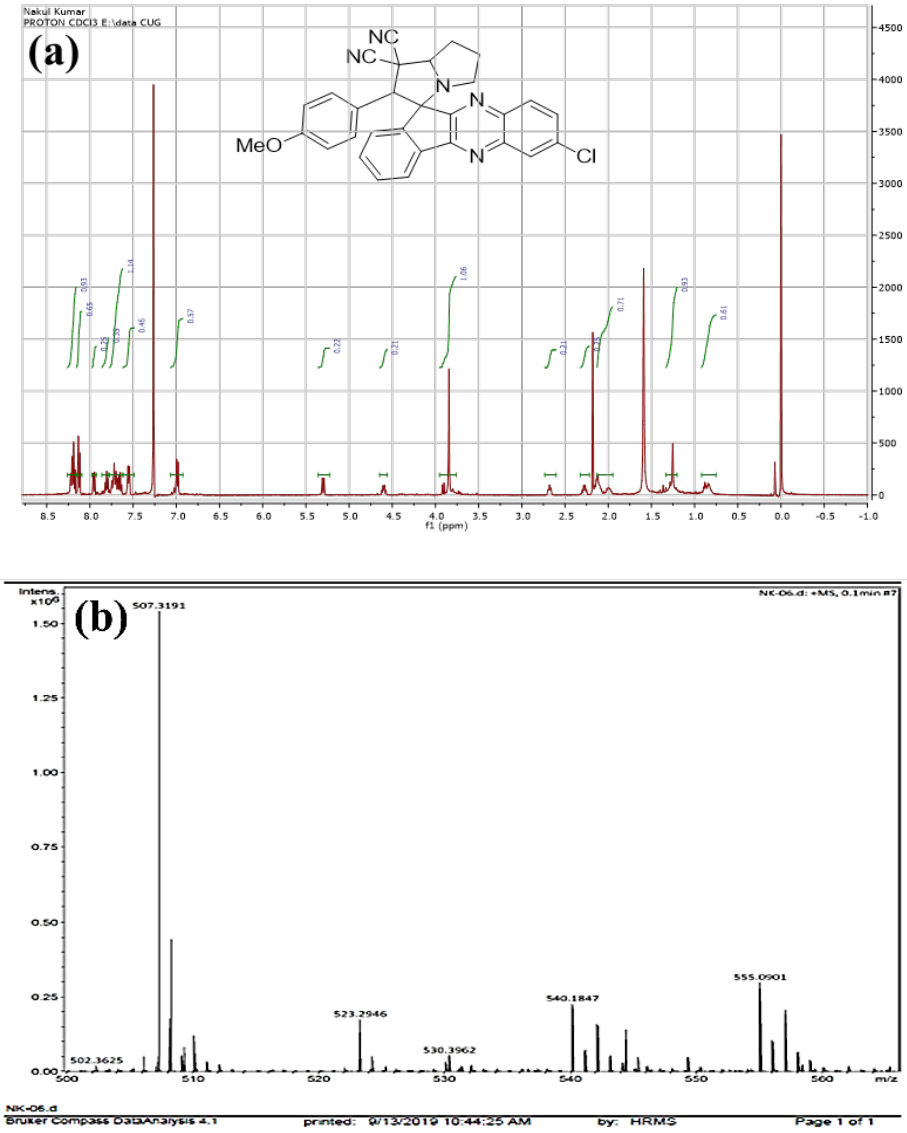

Figure 6. (**a**) 7-chloro-2′-(4-methoxyphenyl)-5′,6′,7′,7a′-tetrahydrospiro[indeno[1,2-b]quinoxaline-11,3′-pyrrolizine]-1′,1′(2′H)-dicarbonitrile and (**b**) MS spectrum for Spiro VI.

Spiro VII: 7-chloro-2′-(3-nitrophenyl)-5′,6′,7′,7a′-tetrahydrospiro[indeno[1,2-b]quinoxaline-11,3′-pyrrolizine]-1′,1′(2′H)-dicarbonitrile: Scheme 8.

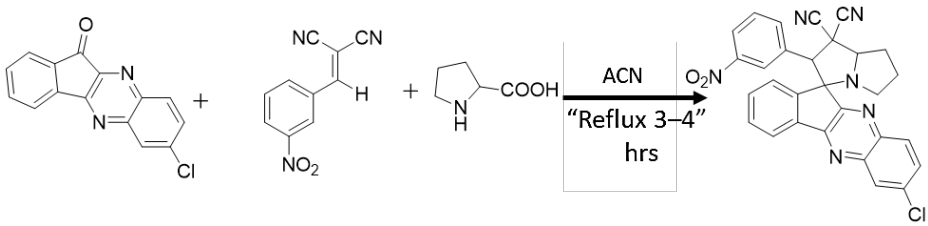

Scheme 8. Synthesis mechanism for 7-chloro-2′-(3-nitrophenyl)-5′,6′,7′,7a′-tetrahydrospiro[indeno[1,2-b]quinoxaline-11,3′-pyrrolizine]-1′,1′(2′H)-dicarbonitrile.

Color, light yellow solid; Yield, 89%,^{1}H-NMR, 500 MHz ($CDCl_3$). The ^{1}H-NMR spectral data of Spiro VII compound is shown in Figure 7a. The obtained values are as follows: δ_H-ppm: 8.86 (s, 1H), 8.47 (d, 1H J = 8.00), 8.34 (d, 1H J = 8.28), 8.21 (m, 1H), 8.18 (d, 1H J = 9.19), 8.12 (d, 1H J = 8.16), 7.95 (d, 1H J = 7.49), 7.81 (d, 1H J = 7.60), 7.77 (s, 1H), 7.75 (d, 1H J = 5.87), 7.71 (d, 1H J = 9.27), 7.65 (d, 1H J = 7.45), 5.48 (d, 1H J = 9.69), 5.31 (s, 1H), 4.66 (d,

1H *J* = 8.31), 2.71 (d, 1H *J* = 7.10), 2.30 (d, 1H *J* = 7.04), 2.05 (s, 1H), 1.38 (s, 1H), 0.87 (d, 1H *J* = 6.50), and the MS, m/z 518.0928, is presented in Figure 7b.

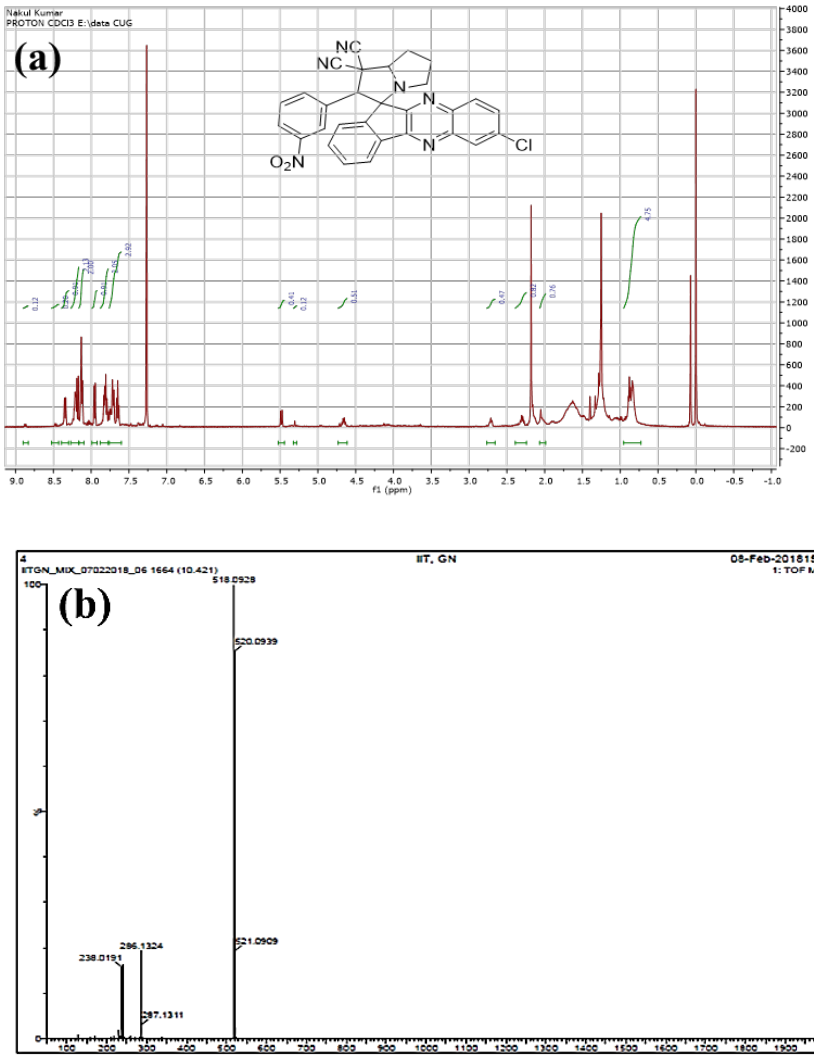

Figure 7. (**a**) 7-chloro-2′-(3-nitrophenyl)-5′,6′,7′,7a′-tetrahydrospiro[indeno[1,2-b]quinoxaline-11,3′-pyrrolizine]-1′,1′(2′H)-dicarbonitrile and (**b**) MS spectrum for Spiro VII.

Spiro VIII: 7-chloro-2′-(4-cyanophenyl)-7′,7a′-dihydrospiro[indeno[1,2-b]quinoxaline-11,3′-pyrrolizine]-1′,1′(2′H)-dicarbonitrile, Scheme 9.

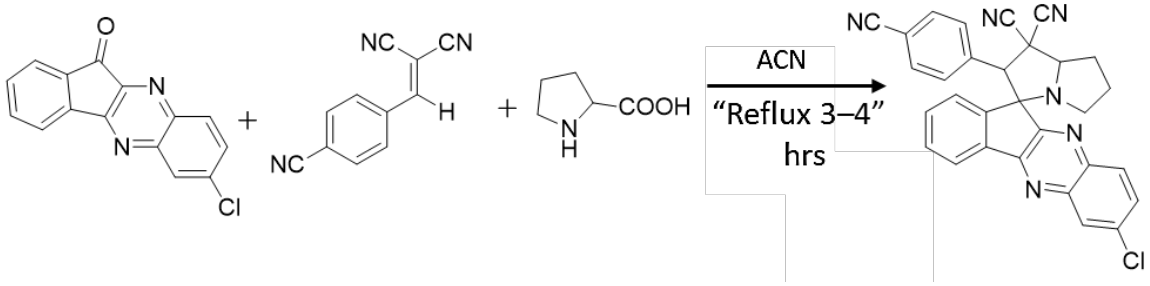

Scheme 9. Synthesis mechanism for 7-chloro-2′-(4-cyanophenyl)-7′,7a′-dihydrospiro[indeno[1,2-b]quinoxaline-11,3′-pyrrolizine]-1′,1′(2′H)-dicarbonitrile.

Color, light yellow solid; Yield, 91%; ^{1}H-NMR, 500 MHz ($CDCl_3$). The ^{1}H-NMR spectral data of Spiro VIII compound is shown in Figure 8a. The observed structural NMR

parameters are as follows: δ_H-ppm: 8.34 (d, 1H *J* = 8.18), 8.30 (d, 1H *J* = 8.29), 8.20 (s, 1H), 8.17 (s, 1H), 8.13 (d, 1H *J* = 8.43), 8.09 (t, 1H *J* = 7.45), 7.95 (d, 1H *J* = 7.58), 7.82 (m, 1H *J* = 6.56), 7.77 (s, 1H), 7.73 (d, 1H), 7.65 (t, 1H *J* = 7.49), 7.13 (d, 1H *J* = 7.79), 5.48 (d, 1H *J* = 9.61), 5.30 (s, 1H), 4.95 (d, 1H *J* = 5.34), 4.65 (m, 1H *J* = 8), 4.55 (d, 1H *J* = 5.53), 4.36 (s, 1H), 4.12 (d, 1H *J* = 7.46), 3.99 (d, 1H *J* = 11.08), 3.30 (s, 1H), 2.71 (s, 1H), 2.32 (s, 1H), 2.05 (s, 1H), 0.87 (d, 1H *J* = 6.68). The MS, m/z 496.1838 (m ± 2), is shown in Figure 8b.

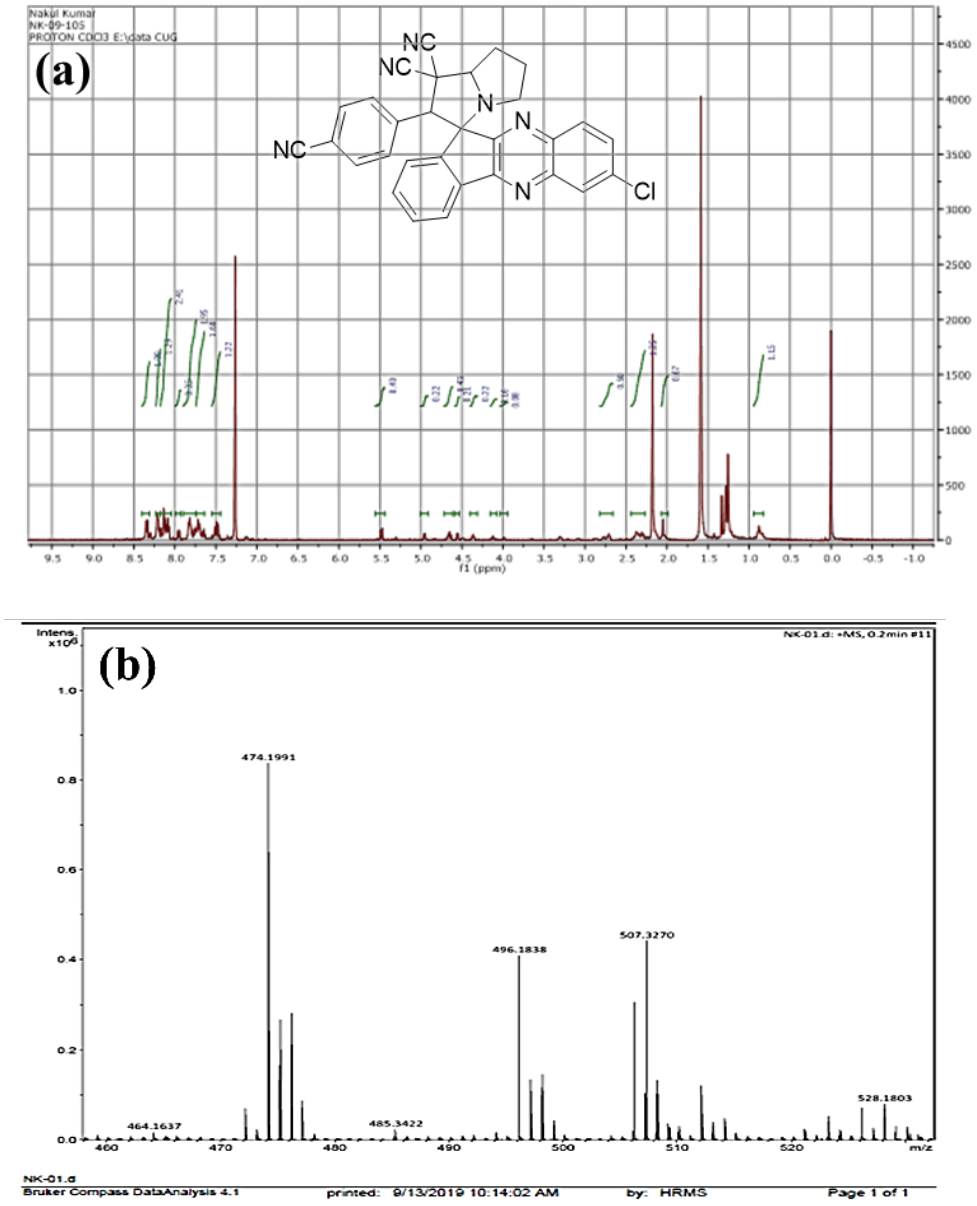

Figure 8. (**a**) 7-chloro-2′-(4-cyanophenyl)-7′,7a′-dihydrospiro[indeno[1,2-b]quinoxaline-11,3′-pyrrolizine]-1′,1′(2′H)-dicarbonitrile and (**b**) MS spectrum for Spiro VIII.

2.2. FTIR Spectral Analysis of Spiro Pyrrolizidines Derivatives

To identify the various functional groups involved in synthesized heterocyclic Spiro compounds, the FTIR technique was performed, and the spectra were taken at room temperature (25 °C). Spiro I: stretching vibrational frequency of the functional groups (–CH, –CN, –CH_3, –C–Cl) appeared at around 2850, 2250, 1450, and 800 cm^{-1}, respectively, as shown in Figure 9a. Spiro II: stretching vibrational frequency of the functional groups (–C–F, –CN, –CH_3, –C–Cl) appeared at around 1350, 2250, 1450, and 800 cm^{-1}, respectively, as shown in Figure 9b.

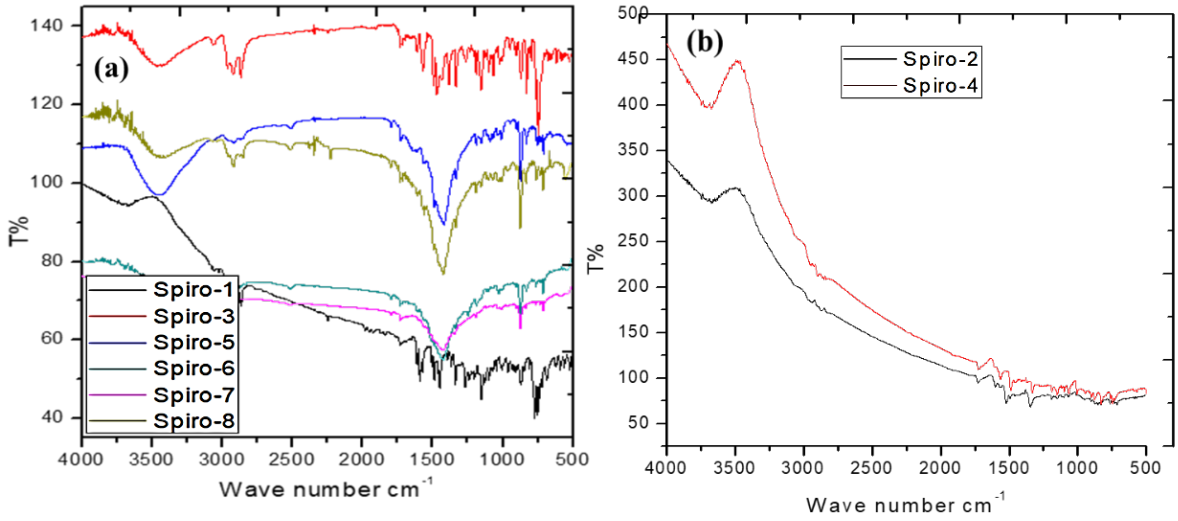

Figure 9. FTIR Spectra: (**a**) Spiro compounds (I, III, V, VI, VII, and VIII) and (**b**) for (II and IV).

The peaks at around 750, 2250, 1450, and 800 cm^{-1} indicate the presence of the Spiro III compound's functional groups (–C–Br, –CN, $–CH_3$, –C–Cl) (Figure 9a). The confirmation of the (–C–Br, –CN, $–CH_3$, –C–Cl) functional groups were assigned for the Spiro IV compound at 750, 2250, 1450, and 800 cm^{-1} frequencies, respectively (Figure 9b). Further, the Spiro V stretching vibrational frequencies of the functional groups (–C–Cl, –CN, –CH, –CH) exist at 800, 2250, 1450, and 3300 cm^{-1}, shown in Figure 9a. while the Spiro VI stretching frequency of the functional groups (–C–CH_3, –CN, –C–Cl) are found at 2950, 2250, and 800 cm^{-1}, as shown in Figure 9a. The Spiro VII compound showed its stretching frequency at 1400, 2250, 1450, and 800 cm^{-1} for the functional groups (–C–NO_2, –CN, $–CH_3$, –C–Cl) (Figure 9a) and the Spiro VIII compound showed its stretching frequency at 2250, 1450, and 800 cm^{-1} for the functional groups (–CN, $–CH_3$, –C–Cl), as shown in Figure 9a. It is noted that systems II and IV showed different behavior due to the involvement of electron-withdrawing functional groups, confirmed by the FTIR. Meanwhile, except for these two systems, I, III, V, VI, VII, and VIII showed the same manners due to the electron-donating function components.

3. Biological Activities

Antimicrobial studies were carried out for Gram-positive *S. aureus*, *B. megatherium*, and *B. subtilis*, and for Gram-negative *E. coli*, *S. typhi*, and *A. aerogenes* organisms using sterile Media under the Disc Diffusion Method. A zone of inhibition of the synthesized compounds was noted and compared with the standard drug Norfloxacin. The entire work was carried out, followed by a horizontal Laminar Flow Hood [16]. The IC_{50} value corresponded to the concentration required for 50% inhibition. The inhibition efficiency is calculated following Equation (1).

$$\text{Percent Inhibition} = \frac{\text{Rate without Inhibitor} - \text{Rate with inhibitor}}{\text{Rate without Inhibitor}} \times 100 - 1 \quad (1)$$

3.1. Antimicrobial Activities Evaluation

The Samples were solubilized in DMSO and soaked into 6 mm sterile discs to achieve final concentrations of 1 mg/disc for antimicrobial assay. The samples were screened against various strains of *S. aureus*, and the results were expressed as a zone of inhibition (in mm). We have examined antimicrobial studies of synthesized compounds and it has shown excellent performance as an antimicrobial agent, as shown in Table 1.

Table 1. The minimum inhibitory concentration of samples against *S. aureus*.

Sample	MIC (μg/mL)	
	***S. aureus* (MTCC 96)**	**Methicillin-Resistant *Staphylococcus aureus* (MRSA 33)**
1.	125	125
2.	500	500
3.	>500	>500
4.	125	125
5.	500	500
6.	500	500
7.	125	500
8.	125	500
Norfloxacin	62.2	62.5

3.2. Disc Diffusion Assay

The strains of *Staphyloccoccus aureus (*MTCC 96, ATCC 29213, MRSA 33, Sa Cipro, and Sa BRTm) microorganisms were also evaluated in the present study. Each strain of microorganism was grown on infusion agar overnight, and pure colonies were suspended in phosphate buffer saline to achieve a concentration of 0.5 followed by McForland standards. The strain of cell line inhibition efficiency is presented in Table 2. The used method was also performed by several researchers, followed by hybrid metamaterials with different morphologies for the biomedical applications [17,18].

Sterile brain–heart infusion agar plates were taken, and the inoculum was spread-plated to dryness. The sample-impregnated discs were then carefully placed on the seeded plates and left for overnight incubation at 37 °C. Readings were noted on the next day using an antibiotic zone measuring scale, and the result was expressed as a zone of inhibition (mm). The in vitro antibacterial activity was studied using Gram-positive bacteria, and also *Staphylococcus aureus* (ATCC 29213), *Staphylococcus aureus* (MTCC 96), and MRSA 33, Sa Cipro, and Sa BRT. The known antimicrobial agent Norfloxacin (reference antibacterial drugs) has been studied for differentiating the antimicrobial activity of Spiro pyrrolizidines.

Table 2. Cell lines inhibition efficiencies for different strains.

Sample	MTCC 96	ATCC 29213	MRSA 33	Sa Cipro	Sa BRT
1.	8	5	8	5	0
2.	3	0	3	0	2
3.	0	3	0	2	0
4.	7	0	8	0	0
5.	6	0	5	5	6
6.	5	4	4	2	1
7.	7	0	6	1	0
8.	8	2	7	4	5
Norfloxacin	10	10	10	10	10

It was evaluated that the tested compounds are more effective against Gram-positive bacteria. The Spiro pyrrolizidines are important derivatives/factors for interactions with biological systems. Several methods were proposed to investigate the drug molecules using cross biological membranes. Lipophilicity also has an important parameter, due to its contribution to absorption, distribution, metabolism, excretion, and toxicity of drug molecules. The hydrophobic drug molecules are significantly adsorbed on the lipid cell wall, but only in cases where the hydrophilic drug molecules could have interacted with blood serum. Hydrophobicity and lipophilicity are important factors for interaction with the

body environment and during removal from the body cells. For this reason, we have designed spiro pyrrolizidine compounds to overcome the recent problem. In general, protein molecules bind with the hydrophobic active sites. In Spiro, pyrrolizidine derivatives are slightly soluble in a non-polar solvent, which could increase the lipophilicity due to the functional groups present in the structure. Synthesized spiro derivatives possess excellent actives sides, such as C=N–C–R (R = Br, F, Cl, O, Me, CN, NO_2). The halogen families are excellent leaving groups and could make carbocation, and the cation side could be able to interact with cell walls. According to MIC studies, it has been observed that a lower concentration (4 to 60 mg/mL) of spiro derivatives resulted in higher inhibition efficiency. The biological studies of spiropyrrolizidines on cell lines MTCC 96, ATCC 29213, and MRSA 33 showed excellent inhibition efficiency compared with the cell line Sa CiproSa BRT due to the electron-withdrawing group present in the compound. The amounts of materials and their derivatives are explored for the biomedical, environmental, and optoelectronic impacts along with the organic and polymeric compounds. [19–21].

4. Materials and Methods

4.1. Materials

The required chemicals, such as Ninhydrin, 4-Chlorophenylene 1, 2-diamine, L-Proline, Lithium Bromide, Acetic acid, and DMF, were purchased from Sigma-Aldrich (Darmstadt, Germany) and used for the synthesis reactions without further purification. In the characterization, the possible functional groups present in the synthesized molecules were confirmed by a Perkin Elmer (Santa Clara, California, USA) made Fourier transform infrared (FTIR) model number SP 65. The ^{1}H-NMR analysis was carried out using a Bruker AVANCE III HD 500 MHz spectrometer (Alberta, Canada), and the TMS reference sample was used as an internal standard, in $CDCl_3$ as a solvent. The NMR spectral data were analyzed in ppm units. The Mass spectral data were recorded by an Agilent Technologies 6545 Q-TOF LC/MS (Santa Clara, California, USA), and methanol was used as a moving solvent.

4.2. Synthesis Procedure for Starting Materials

The starting material was synthesized by a one-step method using malononitrile and aldehyde with lithium bromide (catalytic amount) and dimethyl formamide (DMF) as a solvent. The reaction conditions are presented in Table 3. The taken reaction mixture was stirred for 1 h at room temperature, and the reaction was monitored by TLC. After completion of the reaction, the product was quenched, adding ice, and then filtered using Whatmann (Ontario, Canada) filter paper (Scheme 10).

Table 3. Reaction parameters of starting materials.

Sr. No.	Chemical Name	Molecular Weight	Mmol	Quantity	Equivalent
1.	Malononitrile	66.06	100	6.6 gm	1
2.	Aldehyde	-	100	-	1
3.	Lithium Bromide	86.84	Catalytic amount	50 mg	-
4.	DMF (Solvent)	-	-	20 mL	-

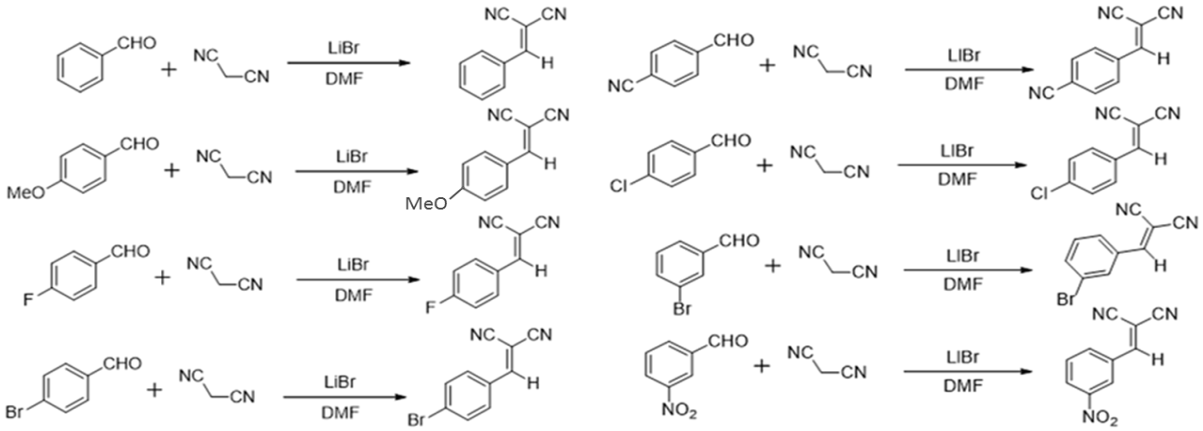

Scheme 10. Synthesis of starting materials.

4.3. Synthesis of 7-Chloro-11H-Indeno[1,2-b]Quinoxaline

A mixture of 4-Chlorobenzene-1,2-diamine (2.34 gm, 15 mmol, 1.1eq) and Ninhydrin (2.672 gm, 15 mmol, 1eq) were added to acetic acid (10 mL) and methanol (30 mL), in a 1:3 ratio, as solvent. A continuously stirred condition was maintained to propagate the reaction, and the mixture was then refluxed for 1 h, which yielded approximately 3.91 gm of product (Scheme 11a). The ^{1}H-NMR spectra were recorded for the 7-chloro-11*H*-indeno[1,2-b]quinoxaline starting materials (Scheme 11b). The product was found to be pale yellow powder (yield: 95%), ^{1}H-NMR 500 MHz (CDCl3) δ: Aromatic protons 9.13 (s, 1H), 8.61 (d, 1H, *J* = 9.46 Hz), 8.29 (d, 1H, *J* = 9 Hz), 8.20 (d, 1H, *J* = 7.50 Hz), 8.02 (d, 1H, *J* = 7.41 Hz), 7.87 (t, 1H, *J* = 7.28 Hz), 7.73 (t, 1H, *J* = 7.41 Hz). The optimized reaction conditions are presented in Table 4. The reaction was monitored by Thin Layer Chromatography (TLC). The precipitate formed was filtered and washed using MeOH (3 times) for normal conditions. The yellow product was dried under a vacuum oven at 50 °C for 24 h.

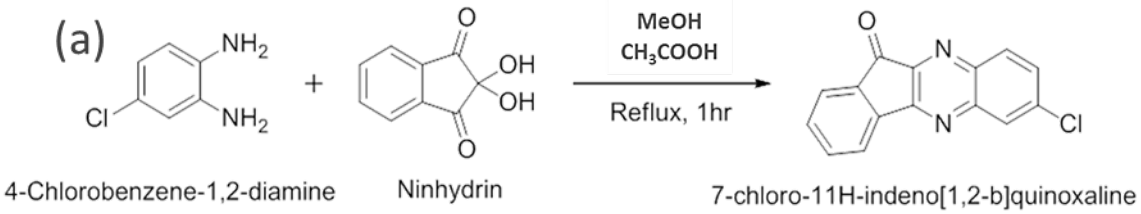

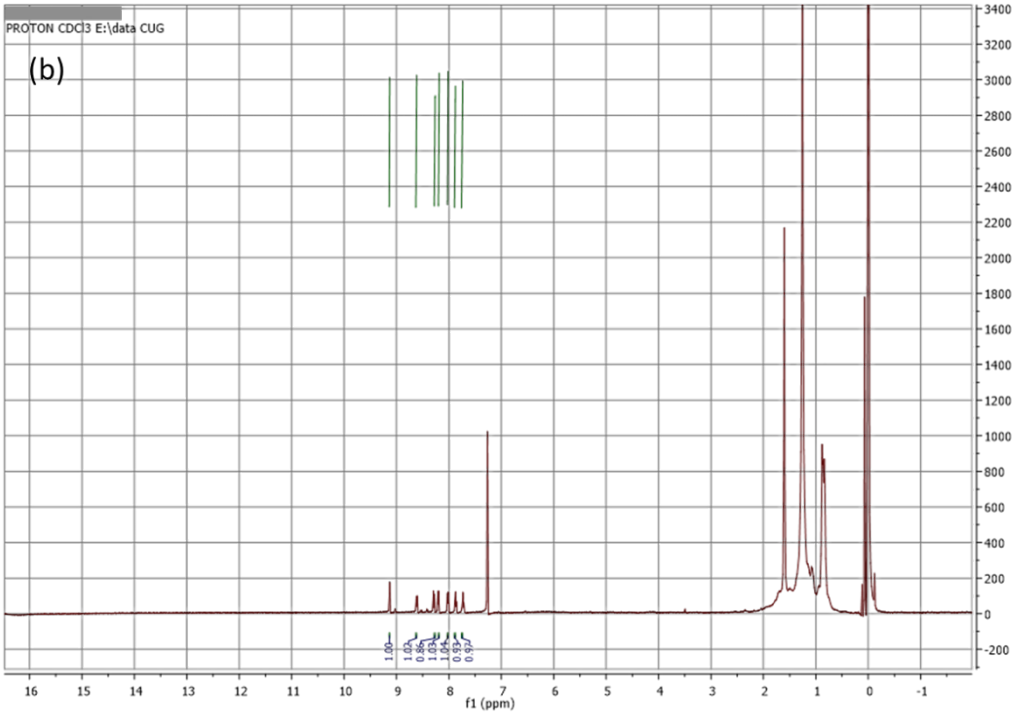

Scheme 11. (**a**) Synthesis of 7-chloro-11H-indeno[1,2-b]quinoxaline, (**b**) ^{1}H Spectra for 7-Chloro-11H-indeno[1,2-b]quinoxalin-11-one.

Table 4. Reaction parameters of 7-chloro-11H-indeno[1,2-b] quinoxaline.

S. No.	Chemical Name	Mol. Weight	Mmol	Quantity	Equivalent
1.	4-Chlorobenzene-1,2-diamine	142.58	15	2.34 gm	1.1eq
2.	Ninhydrin	178.14	15	2.67 gm	1eq
3.	Acetic acid	60.05		10 ml	
4.	MeOH			30 ml	

4.4. Synthesis of Spiro-Pyrrolizidines

In a sequence, 2-benzylidenemalononitrile (154 mg), 1eq and L-proline (127 mg) 1.1eq; 2-(4-fluorobenzylidene) malononitrile (171 mg), 1eq and L-proline (127 mg) 1.1eq; 2-(3-bromobenzylidene) malononitrile (232 mg), 1eq and L-proline (127 mg) 1.1eq; 2-(4-bromobenzylidene) malononitrile (232 mg), 1eq and L-proline (127 mg) 1.1eq; 2 (4chloro-benzylidene) malononitrile (188.6 mg), 1eq and L-proline (127 mg) 1.1eq; 2-(4-methoxybenzylidene) malononitrile (184 mg), 1eq and L-proline (127 mg) 1.1eq; 2-(3-nitrobenzylidene)malononitrile (199 mg), 1eq and L-proline (127 mg) 1.1eq; 2-(4-cyanobenzylidene) malononitrile (179.18 mg), 1eq and L-proline (127 mg) 1.1eq precursors were used, along with a fixed amount of 1,7-chloro-11H-indeno[1,2-b]quinoxalin-11-one (266 mg) 1eq. The starting material in 10 mL acetonitrile was placed in a round bottomed flask for the preparation of the I–VIII Spiro compounds (Table 5). The reaction was stirred and refluxed for 3–4 h, until the reaction mixture became homogeneous. The reaction mixture was broken up by DCM (3 times) and washed by lime water. The molecules were isolated and purified by column chromatography (Scheme 12).

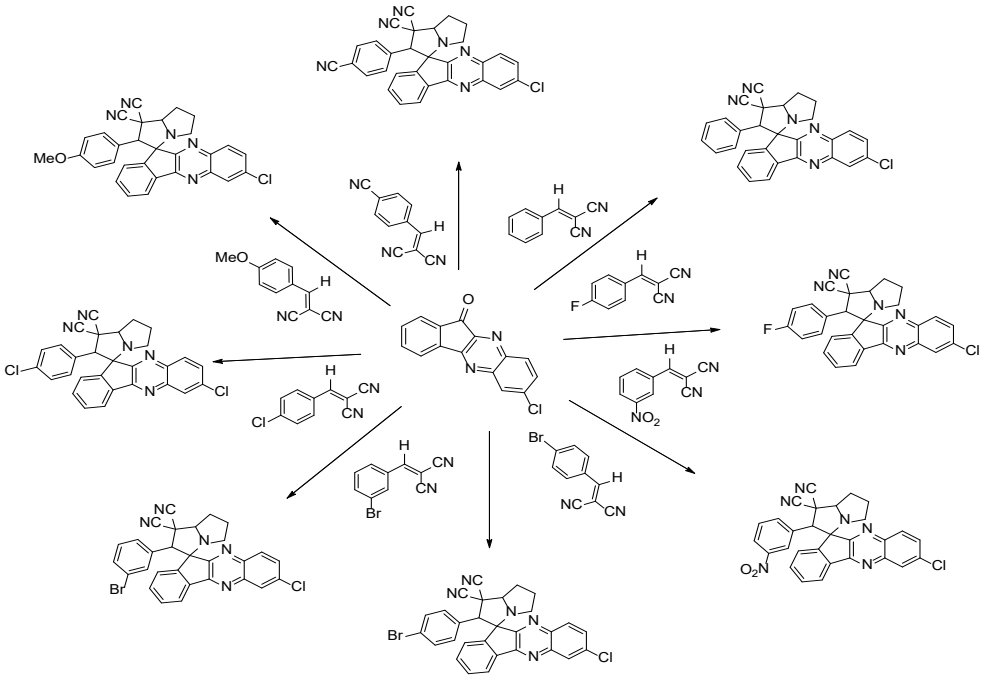

Scheme 12. Schematic representation for Spiro I–VIII compounds.

Table 5. 7-chloro-2′-phenyl-7′,7a′-dihydrospiro[indeno[1,2-b]quinoxaline-11,3′-pyrrolizine]-1′,1′(2′H)-dicarbonitrile.

S. No.	Chemical Name	Mol. Weight	Mmol	Quantity	Equivalent
1.	7-chloro-11H-indeno[1,2-b]quinoxalin-11-one	266	1	266 mg	1eq
2.	Starting material	-	1	-	1eq
3.	L-Proline	115	1	126.5 mL	1eq
4.	ACN			10 L	

4.5. Microbroth Dilution Assay

The 96-well micro-fiber plates (Merck, Darmstadt, Germany) were taken under sterile conditions; 100 µL of broth was dispensed in all wells, except the first column, where 150 µL was dispensed. A fixed 50 µL of each sample (10 mg/mL) was added to the first column of the plate. Two-fold serial dilution was then made up to the last well. An inoculum of 10 µL was added to all wells. Suitable controls, such as only broth, broth + inoculum, were also taken. The plates were incubated overnight at 37 °C, and the readings were noted after 24 h. It was observed that no turbidity was considered by dilution for MIC. Furthermore, the corresponding concentration was calculated in order to decode the exact minimum inhibitory concentration of the samples, which was expressed in µg/mL units.

5. Conclusions

Spiro indinoquinoxaline pyrrolidines and a series of derivatives were synthesized by one-pot reaction using 1,3-dipolar cycloaddition. The characteristic chemical components were confirmed by ^{1}H-NMR, FTIR, and Mass spectral analysis. A maximum yield of 97% was obtained for the synthesized Spiro compounds/derivatives. The characteristic vibrational stretched frequencies revealed the presence of functional groups for the different derivatives. Based on biological studies, Spiro derivatives have shown active inhibition and a maximum efficiency of 50% against Gram-positive species. The antimicrobial studies showed significant results on MTCC 96, ATCC 29213, MRSA 33, Sa Cipro, and Sa BRT cell lines due to functionalized chemical groups. The biological results have shown an

efficient impact due to the involvement of active spiroindinoquinoxalinepyrrolidine biding sites. The electron-donating or withdrawing binding sites mainly interact with the biological molecular structures due to the lipophilic interaction, and hence showed a potential application in the biomedical sectors. These functionalized Spiro pyrrolidine structures could be explored regarding various antibacterial/microbial species as synthetic Spirocyclic agents. However, the structural and physicochemical properties of such spirocyclics could be manipulated by exchanging the active sites with desired functional components with the aim of producing targeted applications.

Author Contributions: Conceptualization, N.K., G.K.I., C.L. and H.-J.A.; Data curation, G.K.I., S.I., C.L. and N.K., methodology, N.K., G.K.I., E.M.A., C.L., H.-J.A. and B.-H.J.; validation, K.K.Y., S.I., C.L., B.-H.J. and V.K.Y.; formal analysis, N.K., G.K.I. and C.L.; resources, K.K.Y., B.-H.J. and S.I.; writing—original draft preparation, N.K., G.K.I. and C.L.; writing—review and editing, N.K., G.K.I., B.M., C.L., E.M.A. and H.-J.A.; supervision, C.L., H.-J.A., S.I. and B.-H.J.; project administration G.K.I., V.K.Y., K.K.Y. and H.-J.A.; Funding acquisition, B.-H.J., S.I., H.-J.A. and E.M.A.; Investigation, N.K., V.K.Y. and B.-H.J.; Software's, G.K.I., K.K.Y. and H.-J.A.; Visualization, G.K.I., V.K.Y., E.M.A. and B.-H.J. All authors have read and agreed to the published version of the manuscript.

Funding: Taif University Researchers Supporting Project number (TURSP-2020/84), Taif University, Taif, Saudi Arabia. This work was also supported by the Mid-Career Researcher Program (No. 2020R1A2C3004237) through the National Research Foundation (NRF) of the Republic of Korea.

Acknowledgments: Taif University Researchers Supporting Project number (TURSP-2020/84), Taif University, Taif, Saudi Arabia. This work was also supported by the Mid-Career Researcher Program (No. 2020R1A2C3004237) through the National Research Foundation (NRF) of the Republic of Korea The authors are also thankful to the Central University of Gujarat and the University Grant Commission, New Delhi, for providing financial support through RGNF Scheme No. SC-UTT-11397.

Conflicts of Interest: The authors declare there is no conflict of interest.

References

1. Liu, H.; Dou, G.L.; Shi, D.Q. Regio- and Stereoselective Synthesis of Novel Dispiropyrrolidine Bioxindole Derivatives via Multicomponent Reactions. *J. Comb. Chem.* **2010**, *12*, 292.
2. Yang, J.-M.; Hu, Y.; Li, Q.; Yu, F.; Cao, J.; Fang, D.; Huang, Z.-B.; Shi, D.-Q. Efficient and Regioselective Synthesis of Novel Functionalized Dispiropyrrolidines and Their Cytotoxic Activities, ACS Combinatorial Science. *Am. Chem. Soc.* **2014**, *16*, 139–145.
3. Rahmannejadi, N.; Yavari, I.; Khabnadideh, S. Synthesis and antitumor activities of novel bis-quinazolin-4(3H)-ones. *J. Heterocycl. Chem.* **2020**, *57*, 978–982.
4. Selvakumar, K.; Vaithiyanathan, V.; Shanmugam, P. An efficient stereoselective synthesis of 3-spirocyclopentene- and 3-spiropyrazole-2-oxindoles via 1,3-dipolar cycloaddition reaction', Chemical Communications. *R. Soc. Chem.* **2010**, *46*, 2826–2828.
5. Liu, H.; Dou, G.L.; Shi, D.Q. Regioselective Synthesis of Novel Spiropyrrolidines and Spirothiapyrrolizidines Through Multicomponent 1,3-Dipolar Cycloaddition Reaction of Azomethine. *J. Comb. Chem.* **2010**, *12*, 633.
6. Barkov, A.Y.; Zimnitskiy, N.S.; Korotaev, V.Y.; Kutyashev, I.B.; Moshkin, V.S.; Sosnovskikh, V.Y. Regio- and stereoselective 1,3-dipolar cycloaddition of indenoquinoxalinone azomethine ylides to β-nitrostyrenes: Synthesis of spiro[indeno[1,2-b]quinoxaline-11,3′-pyrrolizidines] and spiro[indeno[1,2-b]quinoxaline-11,2′-pyrrolidines]. *Chem. Heterocycl. Compd.* **2017**, *53*, 451–459.
7. Huang, Z.; Zhao, Q.; Chen, G.; Wang, H.; Lin, W.; Xu, L.; Liu, H.; Wang, J.; Shi, D.; Wang, Y. An Efficient Synthesis of Novel Dispirooxindole Derivatives via One-Pot Three-Component 1,3-Dipolar Cycloaddition Reactions. *Molecules* **2012**, *17*, 12704.
8. Velikorodov, A.V.; Stepkina, N.N.; Shustova, E.A.; Ionova, V.A. Synthesis of new spiro compounds proceeding from 11H-Indeno[1,2-b]quinoxalin-2-one'. *Russ. J. Org. Chem.* **2015**, *51*, 674–679.
9. Shachkus, A.A.; Degutis, Y.A.; Mikul'skis, P.P. Synthesis of derivatives of 1,3-dihydrospiro[2h-indole-2,2′-pyrrolidine]. *Chem. Heterocycl. Compd.* **1989**, *25*, 47–50.
10. Gothelf, K.V.; Jørgensen, K.A. Asymmetric 1,3-Dipolar Cycloaddition Reactions. *Chem. Rev.* **1998**, *98*, 863.
11. Pattanaik, P.; Nayaka, S.; Ranjan, D.; Pravati, M.; Bishnu, P.; Raigurua, P.; Priyadarsini, N.; Mishraa Mohapatraa, S.; Mallampudib, N.A.; Purohit, C.S. One pot, three component 1,3 dipolar cycloaddition: Regio and diastereoselective synthesis of spiropyrrolidinyl indenoquinoxaline derivatives. *Tetrahedron Lett.* **2018**, *59*, 2688–2694.
12. Lakshmi, N.V.; Thirumurugan, P.; Perumal, P.T. An expedient approach for the synthesis of dispiropyrrolidine bisoxindoles, spiropyrrolidine oxindoles and spiroindane-1,3-diones through 1,3-dipolar cycloaddition reactions. *Tetrahedron Lett.* **2010**, *51*, 1064.

13. Huang, Y.; Huang, Y.-X.; Suna, J.; Yan, C.-G. A [3+2] cycloaddition reaction for the synthesis of spiro[indoline-3,3′-pyrrolidines] and evaluation of cytotoxicity towards cancer cells. *New J. Chem. R. Soc. Chem.* **2019**, *43*, 8903–8910.
14. Tan, W.; Zheng, J.; Guan, J.; Zhan, X.; Gao, L.; Lyu, L.; Shan, B.; Yang, Q.; Ma, M.; Xia, Y. An efficient synthesis of 9-anthrone lactone derivatives via the Knoevenagel condensation and intramolecular cyclization. *J. Heterocycl. Chem.* **2020**, *57*, 1003–1010.
15. Frapper, G.; Bachmann, C.; Gu, Y.; Coval De Sousaa, R.; François, J. Mechanisms of the Knoevenagel hetero Diels-Alder sequence in multicomponent reactions to dihydropyrans: Experimental and theoretical investigations into the role of water. *Phys. Chem. Chem. Phys.* **2011**, *13*, 628.
16. Hana, M.A. Abumelha, Synthesis and antioxidant assay of new nicotinonitrile analogues clubbed thiazole, pyrazole and/or pyridine ring systems., *J. Heterocycl. Chem.* **2020**, *75*, 1011–1022.
17. Inwati, G.K.; Kumar, P.; Roos, W.D.; Swart, H.C. Thermally induced structural metamorphosis of ZnO: Rb nanostructures for antibacterial impacts, Colloids, and Surfaces B. *Biointerfaces* **2020**, *188*, 110821.
18. Malik, P.; Inwati, G.K.; Mukherjee, T.K.; Singh, S.; Singh, M. Green silver nanoparticle and Tween-20 modulated pro-oxidant to antioxidant curcumin transformation in aqueous CTAB stabilized peanut oil emulsions. *J. Mol. Liquids* **2019**, *291*, 111252.
19. Rao, Y.; Inwati, G.; Kumar, A.; Meena, J.; Singh, M. Metal Oxide-based Nanoparticles use for Pressure Sensor. *Int. J. Curr. Eng. Technol.* **2014**, *4*, 2492–2498.
20. Inwati, G.K.; Kumar, P.; Roos, W.D.; Swart, H.C.; Singh, M. UV-irradiation effects on tuning LSPR of Cu/Ag nanoclusters in ion exchanged glass matrix and its thermodynamic behavior. *J. Alloy. Compd.* **2020**, *823*, 153820.
21. Yadav, V.K.; Choudhary, N.; Khan, S.H.; Malik, P.; Inwati, G.K.; Suriyaprabha, R.; Ravi, R.K. Synthesis and Characterisation of Nano-Biosorbents and Their Applications for Waste Water Treatment. In *Handbook of Research on Emerging Developments and Environmental Impacts of Ecological Chemistry*; IGI Global: Hershey, PA, USA, 2020; pp. 252–290.